Aust. J. Phys., 1984, **37**, 509–19

Power and Momentum Relations in Rotating Magnetic Field Current Drive

W. N. Hugrass

School of Physical Sciences, Flinders University of South Australia, Bedford Park, S.A. 5042.

Abstract

The use of rotating magnetic fields (RMF) to drive steady currents in plasmas involves a transfer of energy and angular momentum from the radio frequency source feeding the rotating field coils to the plasma. The power–torque relationships in RMF systems are discussed and the analogy between RMF current drive and the polyphase induction motor is explained. The general relationship between the energy and angular momentum transfer is utilized to calculate the efficiency of the RMF plasma current drive. It is found that relatively high efficiencies can be achieved in RMF current drive because of the low phase velocity and small slip between the rotating field and the electron fluid.

1. Introduction

There has been in recent years a renewed interest in noninductive current drive methods. The realization of a steady state magnetic fusion reactor may well depend on the successful development of a noninductive current drive scheme, since the steady current in a closed plasma equilibrium cannot be maintained using inductive coupling.

Steady currents can be maintained in plasma equilibria by means of neutral beam injection, charged particle beams or r.f. waves (Ohkawa 1970). The r.f. current drive methods can be classified into 'direct methods' and 'indirect methods'. In the direct r.f. current drive methods, the current is maintained by a continuous transfer of momentum to the plasma electrons (Klima 1973). The indirect r.f. current drive methods rely on the creation of an anisotropic collision operator (Fisch and Boozer 1980). The indirect methods will not be considered here since the RMF technique is a direct method.

Fig. 1 illustrates the flow of momentum during r.f. current drive. The r.f. power source generates an r.f. travelling wave field in the plasma. The dissipation (absorption) of the wave energy in the plasma is accompanied by a transfer of directed momentum from the r.f. source to the plasma. In the steady state this momentum must be relaxed to the outside world so that the net gain of momentum is zero. In most r.f. current drive schemes the r.f. fields do not exchange energy (nor momentum) directly with the ions. The momentum balance is approximately given by:

rate of momentum transfer from the r.f. wave to the electrons
= rate of momentum transfer from the electrons to the ions
= rate of momentum transfer from the ions to the outside world.

0004-9506/84/050509$02.00

The electrons absorb energy (and momentum) from the wave by collisional damping or resonant damping (Landau damping, electron cyclotron resonance, Cerenkov absorption etc.). The electrons continuously lose this momentum to the ions via binary collisions or collective or turbulent interactions. Momentum relaxation from the ions to the outside world is caused by atomic processes such as ionization recombination and charge exchange as well as by cross-field diffusion. The rate of momentum transfer to the plasma can also be controlled by the refuelling method (gas puffing, solid pellet, neutral beams etc.).

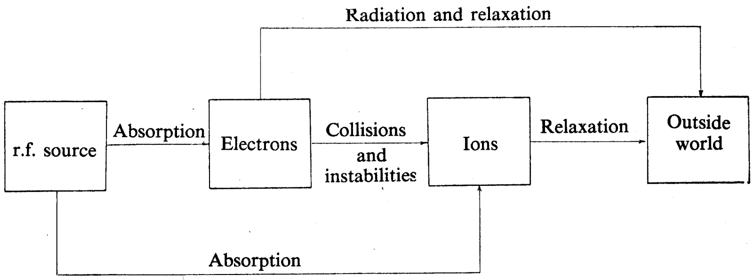

Fig. 1. Flow of momentum during r.f. current drive.

The RMF current drive technique (Blevin and Thonemann 1962; Jones and Hugrass 1981; Hugrass and Grimm 1981; Hugrass *et al.* 1981) is based on the nonlinear phenomenon that conducting fluids are frozen to the lines of force. Consider the situation where the amplitude of the time varying field B_ω and its angular frequency ω are such that

$$eB_\omega/m_i \ll \omega \ll eB_\omega/m_e\,, \tag{1}$$

where e is the electron charge, m_i is the ion mass and m_e is the electron mass. [Note that the condition for current drive (equation 1) does not depend on the equilibrium field (see Hugrass 1982*a*, 1982*b*).] The electron fluid is, in this case, entrained by the travelling wave field whereas the ion fluid is not. A relative motion between the electron and ion fluids takes place, and an electric current is driven provided that two extra conditions are satisfied. Firstly, the wave should travel mainly parallel to the constant density surfaces, and hence the relative motion does not lead to charge separation. Secondly, the collisional friction force between the two fluids should not be so large that it impedes the relative motion: this condition is satisfied provided that

$$\nu_{ei} \ll eB_\omega/m_e\,, \tag{2}$$

where ν_{ei} is the electron–ion momentum transfer collision frequency. It is worth while to mention here that the concept of the conducting fluids being frozen to the lines of force is an oversimplification. The phenomenon under consideration is better described by the more accurate concept of 'flux preserving motion' (Newcomb 1958). The motion of the electron fluid will be flux preserving provided that equations (1) and (2) are satisfied, whereas the motion of the ion fluid does not have to be flux preserving.

This r.f. current drive technique was first utilized to drive a steady current in a toroidal mercury vapour plasma (Thonemann *et al.* 1952). The travelling wave field in this experiment was generated by a helical slow wave structure wound around the torus. Rotating magnetic fields were utilized later to drive steady azimuthal currents in cylindrical plasmas (Blevin and Thonemann 1962; Davenport *et al.* 1966; Blevin and Miller 1965; Hugrass *et al.* 1981). The RMF technique is also used to drive the steady current in the Rotamak configuration which is a compact toroidal equilibrium (Jones 1979; Hugrass *et al.* 1980; Durance *et al.* 1982).

Various aspects of the RMF current drive technique have already been discussed in previous papers (Jones and Hugrass 1981; Hugrass and Grimm 1981; Hugrass 1982*a*; Hugrass and Jones 1983). However, the momentum and power considerations have not been treated with sufficient depth. Fisch and Watanabe (1982) calculated the r.f. power requirements of the RMF current drive using a single particle orbit theory. Their analysis ignored the fundamental interdependence between the energy and momentum transfer (Klima 1973; Hugrass 1982*b*) and they predicted that the efficiency of the RMF current drive technique was much inferior to other r.f. current drive methods. However, a brief analysis based on the work of Klima (1973, 1974) has shown that the efficiency of the RMF current drive compares favourably with that of other techniques (Hugrass 1982*b*).

The purpose of the present paper is to provide a theory for the momentum and energy transfer properties of the RMF technique. The elementary conservation theorems are presented in Section 2 and applied to the RMF current drive. The general properties of RMF systems are discussed in Section 3 where the analogy between the familiar polyphase induction motor and the RMF current drive is explained. The efficiency of the RMF current drive is derived in Section 4 using the Klima theory and the results are discussed in Section 5.

2. General Relationships

The general relationships between the energy and momentum transfer in direct r.f. current drive schemes were first derived by Klima (1973, 1974). A brief derivation of these relationships will be given here because of their utmost importance to the theory of the RMF current drive. The derivation is based on the laws of conservation of energy, momentum and angular momentum:

$$-\oint \boldsymbol{E}\times\frac{\boldsymbol{B}}{\mu_0}.\hat{\boldsymbol{n}}\,\mathrm{d}s=\int_V\left\{\boldsymbol{E}.\boldsymbol{J}+\frac{\partial}{\partial t}\left(\tfrac{1}{2}\varepsilon_0 E^2+\frac{B^2}{2\mu_0}\right)\right\}\mathrm{d}^3r,\tag{3}$$

$$\oint \mathsf{S}.\hat{\boldsymbol{n}}\,\mathrm{d}s=\int_V\left((\rho\boldsymbol{E}+\boldsymbol{J}\times\boldsymbol{B})+\frac{\partial}{\partial t}(\varepsilon_0\boldsymbol{E}\times\boldsymbol{B})\right)\mathrm{d}^3r,\tag{4}$$

$$\oint \boldsymbol{r}\times\mathsf{S}.\hat{\boldsymbol{n}}\,\mathrm{d}s=\int_V\left(\boldsymbol{r}\times(\rho\boldsymbol{E}+\boldsymbol{J}\times\boldsymbol{B})+\frac{\partial}{\partial t}(\boldsymbol{r}\times(\varepsilon_0\boldsymbol{E}\times\boldsymbol{B})\right)\mathrm{d}^3r,\tag{5}$$

where $\boldsymbol{E}\times\boldsymbol{B}/\mu_0$ is the Poynting vector, S is the electromagnetic stress tensor and the surface integrals are carried out over the closed surface bounding the volume V. Note that equations (3)–(5) are derived from Maxwell's equation without any further assumptions. They are quite general and apply to any medium provided that the boundary surface is in a vacuum (free space) region. The components of the stress tensor S are given by

$$S_{ij} = \varepsilon_0 E_i E_j + \mu_0^{-1} B_i B_j - (\tfrac{1}{2}\varepsilon_0 E^2 + \tfrac{1}{2}\mu_0^{-1} B^2)\delta_{ij}. \tag{6}$$

It follows that

$$\mathbf{S}.\hat{\boldsymbol{n}} = \varepsilon_0(\boldsymbol{E}.\hat{\boldsymbol{n}})\boldsymbol{E} + \mu_0^{-1}(\boldsymbol{B}.\hat{\boldsymbol{n}})\boldsymbol{B} - (\tfrac{1}{2}\varepsilon_0 E^2 + \tfrac{1}{2}\mu_0^{-1} B^2)\hat{\boldsymbol{n}}. \tag{7}$$

We now consider the case of a plasma equilibrium to which a r.f. wave field is applied. The equilibrium fields do not contribute to the momentum or energy transfer to the plasma. The average force, torque and power are given by

$$\langle F \rangle = \tfrac{1}{2} \oint \Big(\varepsilon_0(\boldsymbol{E}^*.\hat{\boldsymbol{n}})\boldsymbol{E} + \mu_0^{-1}(\boldsymbol{B}^*.\hat{\boldsymbol{n}})\boldsymbol{B} - (\tfrac{1}{2}\varepsilon_0 \boldsymbol{E}^*.\boldsymbol{E} + \tfrac{1}{2}\mu_0^{-1} \boldsymbol{B}^*.\boldsymbol{B})\hat{\boldsymbol{n}} \Big)\, \mathrm{d}s, \tag{8}$$

$$\langle T \rangle = \tfrac{1}{2} \oint \boldsymbol{r} \times \Big(\varepsilon_0(\boldsymbol{E}^*.\hat{\boldsymbol{n}})\boldsymbol{E} + \mu_0^{-1}(\boldsymbol{B}^*.\hat{\boldsymbol{n}})\boldsymbol{B} - (\tfrac{1}{2}\varepsilon_0 \boldsymbol{E}^*.\boldsymbol{E} + \tfrac{1}{2}\mu_0^{-1} \boldsymbol{B}^*.\boldsymbol{B})\hat{\boldsymbol{n}} \Big)\, \mathrm{d}s, \tag{9}$$

$$\langle P \rangle = -\tfrac{1}{2} \oint \mu_0^{-1}(\boldsymbol{E} \times \boldsymbol{B}^*).\hat{\boldsymbol{n}}\, \mathrm{d}s, \tag{10}$$

where the angle brackets denote time averaging, the asterisk denotes the complex conjugate and the vectors $\boldsymbol{E}$ and $\boldsymbol{B}$ are the complex amplitudes of the r.f. fields.

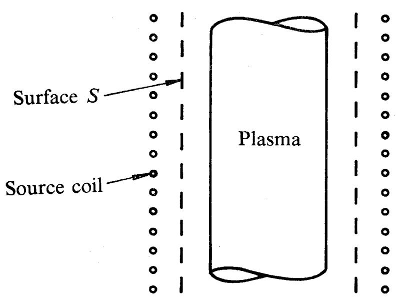

Fig. 2. Schematic diagram for the transfer of linear momentum from a source coil to a plasma cylinder via a travelling wave field.

Klima has considered two important special cases, namely, the case of an infinitely long cylindrical plasma equilibrium (Klima 1973) and that of an axisymmetric equilibrium. Since the z coordinate is ignorable for long equilibria, one may consider a travelling wave field of the form

$$\boldsymbol{E} = E_1(r,\theta)\, \mathrm{e}^{\mathrm{i}(\omega t - kz)}. \tag{11}$$

This travelling wave field can be generated by a source coil placed outside the plasma (see Fig. 2). The surface of integration S is chosen as a cylinder which lies in the vacuum region between the plasma and the source coil. It can be shown using equations (8), (10) and (11) and Maxwell's equations that the power dissipation $\langle P\rangle$ and the rate of transfer of linear momentum $\langle F_z\rangle$ are related by the equation

$$\langle P\rangle = v_{\mathrm{ph}}\langle F_z\rangle, \tag{12}$$

where $v_{\mathrm{ph}} = \omega/k$ is the phase velocity of the travelling wave field (note that it is not the speed of light in free space as has been assumed by several previous authors, see e.g. Ohkawa 1970). Equation (12) is quite general; it does not depend on the dissipation mechanism nor on the nature of the wave.

For axisymmetric equilibria, the coordinate θ is ignorable. The travelling wave field has the form

$$\boldsymbol{E} = E_1(r,z)\,\mathrm{e}^{\mathrm{i}(\omega t - m\theta)}. \tag{13}$$

It has been shown by Klima (1974) that the average rate of transfer of the z component of the angular momentum $\langle T_z\rangle$ is proportional to the average power dissipation $\langle P\rangle$:

$$\langle T_z\rangle = (m/\omega)\langle P\rangle. \tag{14}$$

For the important special case, $m = 1$, one obtains

$$\langle T_z\rangle = (1/\omega)\langle P\rangle. \tag{15}$$

3. General Properties of RMF Systems

In RMF current drive, both energy and angular momentum are transferred from an external circuit to the plasma. The system is closely related to the well known squirrel-cage induction motor. In this section we present the energy–torque relations for a conceptual squirrel-cage motor and for an infinitely long plasma cylinder with RMF current drive, and explain the similarities and the differences between the two systems.

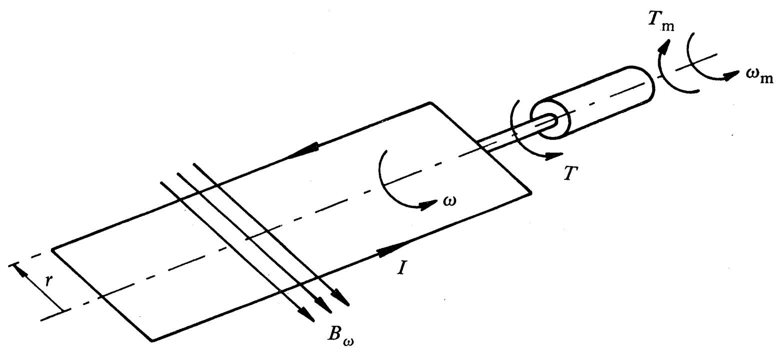

Fig. 3. Schematic diagram for a conceptual induction motor.

Power–Torque Relations in Induction Motors

We consider an idealized conceptual induction motor (Fig. 3). A rotating magnetic field of magnitude B_ω and angular frequency ω is generated by means of a polyphase stator winding (not shown in the figure). The rotor consists of a long single-turn coil which is coupled to a mechanical load. The distance between the axis of rotation and the coil sides is r (i.e. the coil width is $2r$). The coil resistance per unit length is R and its inductance per unit length is L. We assume that the rotor rotates at an average angular frequency ω_m. The slip s is defined as

$$s = (\omega - \omega_m)/\omega . \tag{16}$$

The voltage (per unit length) induced in the coil is

$$V = 2rs\omega B_\omega \tag{17}$$

and consequently the current in the coil is

$$I = 2rs\omega B_\omega/(R^2 + s^2\omega^2L^2)^{\frac{1}{2}} . \tag{18}$$

The torque is given by

$$\langle T\rangle = \tfrac{1}{2}2rB_\omega I\cos\phi , \tag{19}$$

where

$$\phi = \arccos\{R/(R^2 + s^2\omega^2L^2)^{\frac{1}{2}}\} \tag{20}$$

is the phase angle between the current and the magnetic field. It follows that

$$\langle T\rangle = 2Rr^2s\omega B_\omega^2/(R^2 + s^2\omega^2L^2) . \tag{21}$$

The output mechanical power (per unit length) is

$$\begin{aligned}\langle P_m\rangle &= \omega_m\langle T\rangle \\ &= 2Rr^2s(1-s)\omega^2B_\omega^2/(R^2 + s^2\omega^2L^2)\end{aligned} \tag{22}$$

and the power dissipated in the coil resistance is

$$\begin{aligned}\langle P_e\rangle &= \tfrac{1}{2}I^2R \\ &= 2Rr^2s^2\omega^2B_\omega^2/(R^2 + s^2\omega^2L^2) .\end{aligned} \tag{23}$$

The total power transferred to the rotor is

$$\begin{aligned}\langle P\rangle &= \langle P_m\rangle + \langle P_e\rangle \\ &= 2Rr^2s\omega^2B_\omega^2/(R^2 + s^2\omega^2L^2) .\end{aligned} \tag{24}$$

Using equations (21) and (24), we see that

$$\langle T\rangle = (1/\omega)\langle P\rangle ,$$

as predicted by Klima (1974).

It is seen that both the magnetic field and the current in the rotor coil are varying with time. The magnetic force has in general a second harmonic part and a steady part. The steady part vanishes for an ideal coil with zero resistance, since $\cos\phi = 0$ in this case. If the rotor rotates synchronously with the rotating field (zero slip), the e.m.f. induced in the rotor coil will be zero and no rotor current will flow. Consequently the torque is zero for $\omega_m = \omega$. As the slip between the rotor and the field increases, the e.m.f. induced in the rotor coil increases, and so does the effective frequency $s\omega$ and the phase angle $\arctan(s\omega L/R)$. The torque is a maximum for a slip

$$\alpha = R/\omega L. \tag{25}$$

This maximum torque is

$$\langle T\rangle_{\max} = r^2 B_\omega^2/L, \tag{26}$$

while the normalized torque is given by

$$\langle T\rangle/\langle T\rangle_{\max} = 2\alpha s/(\alpha^2+s^2). \tag{27}$$

Fig. 4 shows the variation of the normalized torque with the normalized rotor frequency ω_m/ω for $\alpha = 0{\cdot}2$ and $0{\cdot}4$.

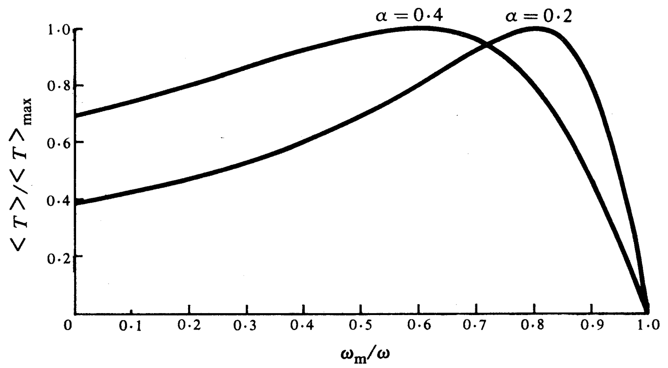

Fig. 4. Normalized torque–angular speed characteristics for an induction motor for $\alpha = 0{\cdot}2$ and $0{\cdot}4$.

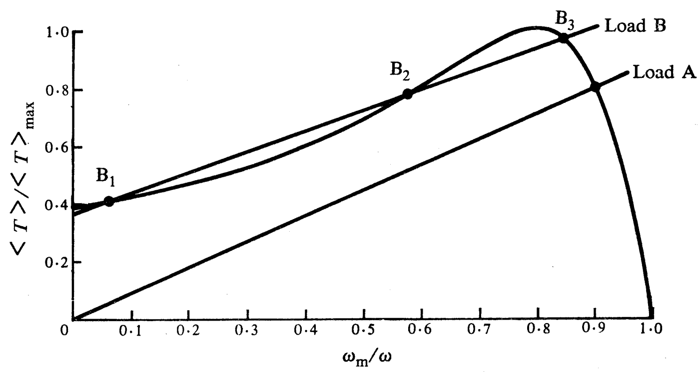

Fig. 5. Example of the use of load lines to determine the operating point for a given motor.

The operating torque and slip are determined by the mechanical load characteristics. Fig. 5 shows the characteristics of a motor with $\alpha = 0{\cdot}2$ together with the characteristics of two hypothetical loads. For load A, the operating point is unique. For load B there are three possible operating points: B_1, B_2 and B_3. Both B_1 and B_3 are stable operating points whereas B_2 is unstable. The motor operating point is either B_1 or B_3 depending on the history of the system.

Power–Torque Relations in RMF Plasma Current Drive

We consider an infinitely long plasma cylinder to which is applied a transverse magnetic field B_ω which rotates about the axis at an angular frequency ω. The rotating magnetic field induces an axial screening current I_z in the plasma cylinder. The azimuthal force acting on the electrons $F_\theta \sim J_z B_r$ has a steady part; consequently, the electrons experience a steady torque. Provided that

$$\nu_{\mathrm{ei}} \ll (m_{\mathrm{i}}/m_{\mathrm{e}})\,\nu^*,$$

where ν_{ei} is the electron–ion momentum transfer collision frequency and ν^* is the effective ion momentum relaxation frequency, the ion fluid can be considered stationary, whereas the electron fluid acquires a steady azimuthal motion (Hugrass 1982*a*). The electron fluid does not rotate synchronously with the field because of the retarding torque produced by collisions with the ions.

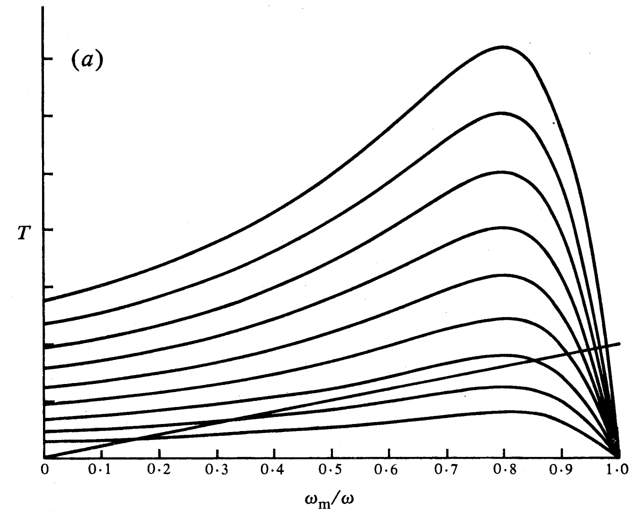

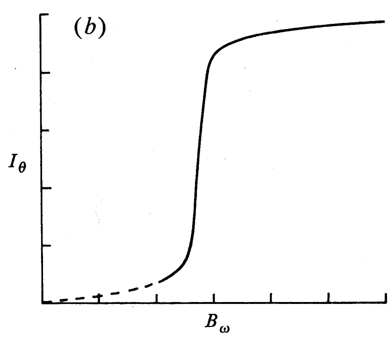

Fig. 6. Schematic diagrams of (*a*) torque–angular speed characteristics for a RMF plasma current drive for different values of the rotating magnetic field amplitude B_ω together with the equivalent load line; (*b*) the corresponding curve of current against field.

It is clear that the electron fluid is analogous to the rotor coil of the induction motor and that the ion fluid is analogous to the mechanical load. Despite the striking similarity, the two systems are not identical. The electron fluid does not in general rotate as a solid body. The slip, therefore, should be regarded as an effective spatial average. It is also meaningless to consider the electron fluid as a lumped *L–R* circuit;

the parameters L and R should be regarded as the equivalent of the distributed impedance of the plasma. The values of L and R depend on the slip because of the skin effect. Nevertheless, the average torque acting on the electron fluid should be (at least qualitatively) given by equation (21) where the equivalent resistance R and the equivalent inductance L are functions of the slip s. The load line is, in this case, very nearly a straight line since the dynamical friction force acting on the electron fluid is approximately proportional to the relative velocity between the electron and ion fluid, provided that the macroscopic velocity is much smaller than the electron thermal velocity.

Fig. 6*a* shows the torque–angular speed characteristics for different values of the rotating field B_ω for a system with $\alpha = R/\omega L = 0{\cdot}2$ (the value of α appropriate to a plasma depends on the ratio of the plasma radius to the classical skin depth). The intersection of the load line with the characteristics for any value of B_ω determines the operating angular speed for the particular value of B_ω. Recalling that the current density is given by

$$J_\theta = -ne\omega_{\mathrm{m}} r\,, \tag{28}$$

one can use Fig. 6*a* to predict the azimuthal current driven in the plasma for any value of B_ω. The curve of I_θ against B_ω, derived from Fig. 6*a*, is shown in Fig. 6*b*. This remarkably nonlinear behaviour was predicted by Hugrass and Grimm (1981) who solved numerically the partial differential equations describing the system. The qualitative nature of the present argument allows a deeper insight into the physical mechanisms involved.

4. Efficiency of RMF Current Drive

We consider a long plasma cylinder in which an azimuthal current is driven by means of a rotating magnetic field. Provided that the ion fluid can be considered stationary, the torque per unit length is

$$T = \int_0^a \nu nmrv_{\mathrm{e}\theta}\, 2\pi r\,\mathrm{d}r\,, \tag{29}$$

where a is the radius of the plasma, ν is the effective electron momentum transfer collision frequency and $v_{\mathrm{e}\theta}$ is the azimuthal velocity of the electron fluid. Using the classical expression for the resistivity

$$\eta = m\nu_0/ne^2\,, \tag{30}$$

where ν_0 is the classical collision frequency, one obtains (with $J_\theta = nev_{\mathrm{e}\theta}$)

$$T = \int_0^a \frac{\nu}{\nu_0} ner\eta J_\theta\, 2\pi r\,\mathrm{d}r\,. \tag{31}$$

The power dissipation per unit length P is obtained by using equations (31) and (15):

$$\begin{aligned} P &= \omega \int_0^a \frac{\nu}{\nu_0} ner\eta J_\theta\, 2\pi r\,\mathrm{d}r \\ &= \int_0^a \gamma\eta J_\theta^2\, 2\pi r\,\mathrm{d}r\,, \end{aligned} \tag{32}$$

where

$$\gamma = (v/v_0)(\omega r/v_{e\theta}). \tag{33}$$

The figure of merit,

$$\langle\gamma\rangle = \int \gamma\eta J_\theta^2\, 2\pi r\, \mathrm{d}r \bigg/ \int \eta J_\theta^2\, 2\pi r\, \mathrm{d}r, \tag{34}$$

is the ratio of the total power transferred to the plasma, to the power dissipation associated with the steady driven current. The 'internal' efficiency $\mathscr{E}_\mathrm{i}$ of the RMF current drive is defined as

$$\mathscr{E}_\mathrm{i} = 1/\langle\gamma\rangle. \tag{35}$$

For RMF current drive, the phase velocity ωr is much smaller than the electron thermal velocity. (For a reactor grade plasma $T_\mathrm{e} \sim 10$ keV and $\omega R \sim 10^5$–$10^6\ \mathrm{m\,s^{-1}}$.) It follows that $v/v_0 \sim 1$. Also the slip between the electron fluid and the rotating field is small: $J_\theta/ne\omega r \lesssim 1$. It follows that $\mathscr{E}_\mathrm{i} \lesssim 1$, i.e. the internal efficiency is of the order 1. This relatively high efficiency is a result of the small slip between the wave field and the electron fluid.

It is seen from equation (33) that higher values of $\mathscr{E}_\mathrm{i}$ can be achieved by maintaining a very small value of the slip s. This corresponds to high values of the rotating field amplitude B_ω. A very large value of B_ω is not desirable for many reasons; it leads to a higher cost of the r.f. source, higher induced voltages, a lower overall efficiency and a larger perturbation to the steady field configuration. It seems that optimum operating conditions correspond to a slip somewhat smaller than that for maximum torque (see Fig. 6*a*). The amplitude of the rotating magnetic field for this operating condition is significantly larger than, but of the same order as, the threshold value (see Fig. 6*b*).

5. Conclusions

The operation of RMF current drive is seen to be closely related to that of the familiar polyphase induction motor. The electron fluid is analogous to the rotor coil and the ion fluid provides the retarding torque and is analogous to the mechanical load. The power–torque relationships are obtained using the general conservation laws following the Klima (1973, 1974) analysis. The efficiency of the RMF current drive is calculated using these results. It is found that the internal efficiency is relatively high; this is brought about by the small slip between the rotating field and the electron fluid.

Acknowledgments

The author acknowledges many discussions with Professor I. R. Jones. This work was supported by the Australian National Energy Research, Development and Demonstration Program.

References

Blevin, H. A., and Miller, R. B. (1965). *Aust. J. Phys.* **18**, 309.

Blevin, H. A., and Thonemann, P. C. (1962). *Nucl. Fusion Suppl.* Part I, 55.

Davenport, P. A., Francis, G., Millar, W., and Taylor, A. F. (1966). Annular plasmas produced by rotating magnetic fields. U.K.A.E.A. Culham Rep. No. CLM-R65.

Durance, G., Jessup, B. L., Jones, I. R., and Tendys, J. (1982). *Phys. Rev. Lett.* **48**, 252.
Fisch, N. J., and Boozer, A. H. (1980). *Phys. Rev. Lett.* **45**, 720.
Fisch, N. J., and Watanabe, T. (1982). *Nucl. Fusion* **22**, 423.
Hugrass, W. N. (1982*a*). *J. Plasma Phys.* **28**, 369.
Hugrass, W. N. (1982*b*). *Nucl. Fusion* **22**, 1237.
Hugrass, W. N., and Grimm, R. C. (1981). *J. Plasma Phys.* **26**, 455.
Hugrass, W. N., and Jones, I. R. (1983). *J. Plasma Phys.* **29**, 155.
Hugrass, W. N., Jones, I. R., McKenna, K. F., Phillips, M. G. R., Storer, R. G., and Tuczek, H. (1980). *Phys. Rev. Lett.* **44**, 1676.
Hugrass, W. N., Jones I. R., and Phillips, M. G. R. (1981). *J. Plasma Phys.* **26**, 465.
Jones, I. R. (1979). The Rotamak concept. Flinders University Rep. No. FUPH-R-151.
Jones, I. R., and Hugrass, W. N. (1981). *J. Plasma Phys.* **26**, 441.
Klima, R. (1973). *Plasma Phys.* **15**, 1031.
Klima, R. (1974). *Czech. J. Phys.* B **24**, 846.
Newcomb, W. A. (1958). *Ann. Phys.* (*New York*) **3**, 347.
Ohkawa, T. (1970). *Nucl. Fusion* **21**, 15.
Thonemann, P. C., Cowhig, W. T., and Davenport, P. A. (1952). *Nature* **169**, 39.

Manuscript received 28 October 1983, accepted 6 August 1984